# MULTIPLE USER BEAM DISTRIBUTION SYSTEM FOR FRIB DRIVER LINAC*

D. Gorelov# , V. Andreev, S. Chouhan, X. Wu, R. C. York,
NSCL/MSU, East Lansing, MI 48824, U.S.A.

*Abstract*

The proposed Facility for Radioactive Ion Beams (FRIB) [1] will deliver up to 400 kW of any stable isotope to Rare Isotop Beam (RIB) production target. Operational efficiency could, under certain conditions, be improved by a system that can distribute the beam current, variable in a large dynamic range, to several independent targets simultaneously. A possible FRIB Beam Switchyard (BSY) utilizes an RF kicker with subsequent magnetostatic septum system to split the beam on micro-bunch to micro-bunch basis. The micro-bunches can be differentially loaded at the front-end of the Driver Linac [2]. The detailed analysis of the beam dynamics performance in the proposed BSY system is presented.

## INTRODUCTION

The effective use of the proposed FRIB facility [1] can under certain conditions be benefited by the ability to support simultaneous experiments. The stable isotope beams from the Driver Linac can be used for production of Radioactive Ion Beams (RIBs) using either Isotope Sepatation On Line (ISOL) or In-flight Particle Fragmentation methods to maximize yield of the corresponding species.

The discussed Beam Switchyard (BSY) will allow separation of the continuous stable ion beam from the Driver Linac into two independent channels on a micro-bunch by micro-bunch basis using an RF kicker followed by magnetic septum system.

The performance of this system was explored in details using three-dimensional electromagnetic fields for the RF kicker and a magnetostatic field distribution in septum magnet. As an alternative to the RF kicker, a DC septum magnet consisting of an array of thin wires and two electrodes can be used for lighter ions.

## BEAM SWITCHYARD (BSY) SYSTEM

A proposed FRIB BSY design uses an RF kicker, an alternative DC bending dipole, and a septum magnet along the beam transport channel to either split the incoming stable beam into two beam lines with 50% intensity in each branch or to supply a single target with the full beam intensity (100 %) any of two production targets. The intensity of the two branches can be varied from 0% to 50% total beam intensity independently using the additional system of differential beam loading [2]. Figure 1 shows the layout of the proposed BSY system.

To minimize beam loss, quadrupole magnets in front of the RF kicker are provided to achieve reduced horizontal beam size at the entrance of the septum magnet. Both the RF kicker and the DC dipole have the same design deflection angle of ±1.5 mrad and will be used interchangeably for either splitting the incoming beam into two segments or direct all beam into one of the following beam lines. Given the beam micro-bunch frequency of 80.5 MHz, an RF kicker frequency of 120.75 MHz is appropriate to split the beam into two segments by kicking every other bunch in opposite transverse directions. A 10 m long drift space after the initial splitting point in RF kicker is required to generate enough spatial separation to accommodate a 10 mm thick septum in the septum magnet.

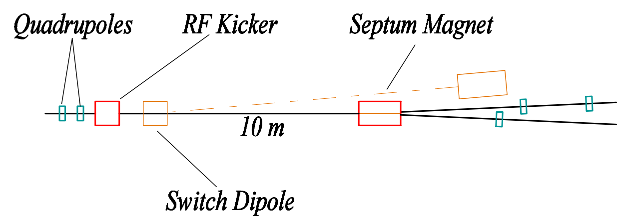


Figure 1: Layout of a proposed FRIB BSY system.

The performance of the proposed BSY system was evaluated by detailed beam dynamics simulations using the realistic three-dimensional (3D) distributions of the electromagnetic RF and magnetostatic fields in the system elements.

### *RF Kicker*

The electromagnetic (EM) field calculations for the RF kicker were done using the computer code MAFIA. The resonant structure of the RF kicker is shown in Figure 2 and represents a “lumped circuit” consisting of two parallel plates (capacitance) and four stems (inductors).

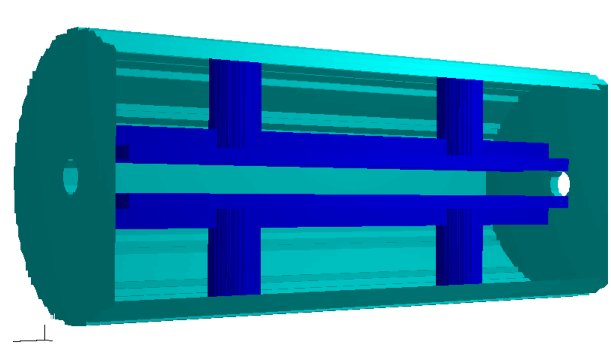

Figure 2: Three-dimensional view of the RF kicker.

The transverse electric field created between the plates deflects the beam in the direction perpendicular to the planes and parallel to the stems. Using two stems improves stiffness of the structure, simplifies cooling, and helps to equalize the longitudinal electric field

*Work was supported by the US DOE grant DE-FG02-04ER41324.
#gorelov@msu.edu

distribution. Selected parameters of the RF kicker are listed in Table 1.

Table 1: RF Kicker Structure Parameters

| | |
|---|---|
| Beam bunch frequency | 80.5 MHz |
| RF kicker harmonic | 3/2 |
| RF kicker frequency | 120.75 MHz |
| Deflection angle | ±1.5 mrad |
| RF power | 28 kW |
| RF voltage | 170 kV |
| Tank diameter | 0.4 m |
| Stem diameter | 0.08 m |
| Plate width | 0.12 m |
| Plate thickness | 0.02 m |
| Plate length | 0.88 m |
| Gap | 0.05 m |

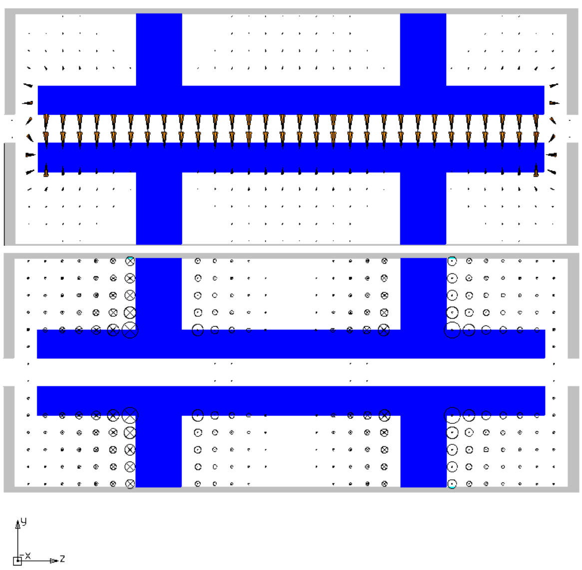

Figure 3: Electric (top) and magnetic (bottom) field distribution in a central vertical cross-section along the beam axis of the RF kicker structure.

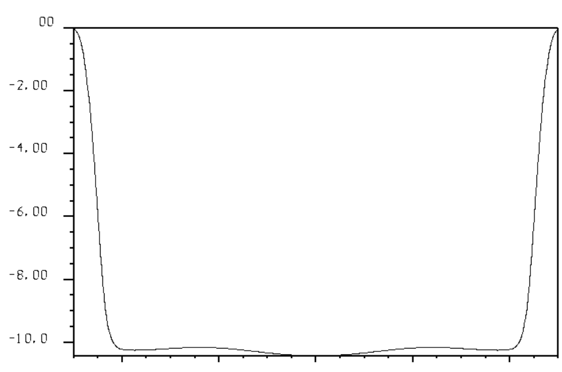


Figure 4: Transverse electric field profile in the RF kicker along the beam axis.

Electric and magnetic field distributions of the resonant structure are shown in Figure 3. Transverse electric field has variance of less then 5 % on the 80 cm of total effective length of the RF kicker deflecting plates as shown in Figure 4. Transverse electric field in the Extent of the direction orthogonal to the beam direction and plane of deflection has a variance of less then 1 % over a width of ± 4 cm Power dissipation inside the resonant structure versus inter-plate voltage is shown in Figure 5.

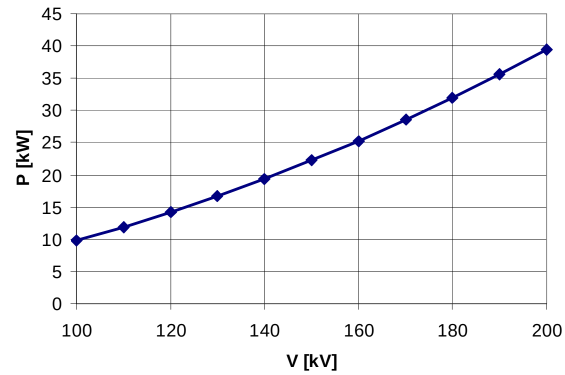


Figure 5: RF power losses in the structure vs. inter-plate voltage.

### *Septum Magnet*

The magnetic field of the septum magnet was modeled using the OPERA computer code. Table 2 lists the main parameters of the septum magnet. Figure 6 shows the 3D view of septum magnet.

Table 2: Septum Magnet Main Parameters

| | |
|---|---|
| Septum thickness | 0.16 m |
| Bending angle | ±2.5 ° |
| Full gap | 0.062 m |
| Peak field | 0.22 T |
| Excitation current | 5500 A |
| Current density | 3000 A/cm$^2$ |
| Effective length | 1.814 m |
| Coils cross-section | 30 mm x 6 mm |

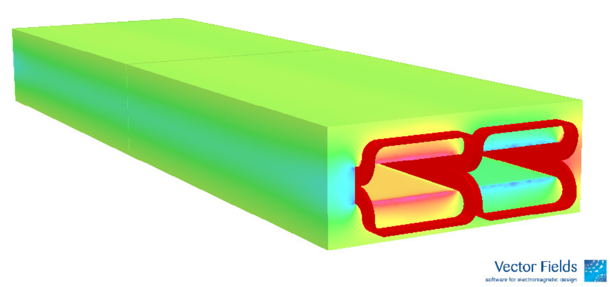


Figure 6: Three-dimensional view of the septum magnet.

## BEAM DYNAMICS SIMULATION RESULTS

Beam dynamics analysis of the proposed BSY was done using the LANA code [3]. The detailed analysis of the beam dynamics in the septum magnet was also done in parallel using the KOBRA code. The results from KOBRA and LANA were found to be in agreement within model accuracy. In all simulations, the three-dimensional electromagnetic field of the RF kicker and the magnetostatic field of septum magnet were used with the field distributions obtained from the MAFIA and OPERA computer codes respectively.

The initial beam parameters obtained from end-to-end beam simulations for the driver linac used in the BSY simulation are given in Table 3. Four quadrupole magnets before the RF kicker were used to obtain the required beam phase space at the RF kicker entrance.

Table 3: BSY Input Beam Parameters

| | | | |
|---|---|---|---|
| Energy | 400 MeV/u | $\varepsilon_Z$ | 27.6 $\pi$ ns keV/u |
| Q | 89+ | $\alpha_Z$ | 0 |
| A | 238 | $\beta_Z$ | 20.0 degree/% |
| $\varepsilon_X$ | 1.6 $\pi$ mm mrad | $\varepsilon_Y$ | 1.6 $\pi$ mm mrad |
| $\alpha_X$ | 0 | $\alpha_Y$ | 0 |
| $\beta_X$ | 1.0 | $\beta_Y$ | 1.0 |

The RF kicker is used to create an initial spatial separation between sequential (every other) bunches. To deflect every other bunch into two different trajectories, the operating frequency of the rf kicker can be any odd half-integer of the bunch frequency. The 3/2 harmonic, which corresponds to a frequency of 120.75 MHz, was chosen (see Table 1).

The septum magnet is used to further separate two beams in space. The septum magnet is placed 10 meters downstream the RF kicker where the two beams are sufficiently separated. The main beam dynamics parameters of the septum magnet are given in Table 2.

The resulting separation of the beam bunches in the bending plane for the design settings of the system parameters are summarized in the Table 4.

Table 4: Bunch Separation in the Bending Plane

| Separation | After RF kicker | Before septum | After septum |
|---|---|---|---|
| x (±) [mm] | 0.8 | 15.7 | 73.1 |
| x` (±) [mrad] | 1.53 | 1.53 | 48.5 |

Table 5: Estimation of the Total Emittance Growth in the BSY

| Relative emittance growth [%] | After RF kicker | At the end of BSY |
|---|---|---|
| $\delta\varepsilon_X/\varepsilon_X$ | <0.1 | ~2.0 |
| $\delta\varepsilon_Y/\varepsilon_Y$ | 0 | <0.5 |
| $\delta\varepsilon_Z/\varepsilon_Z$ | 0 | 0 |

From simulation, the effective emittance growth in the proposed BSY was negligible except in the bending plane. The variation of the emittance in the other planes was comparable to the simulation model accuracy. The summary of the emittance growth is given in the Table 5. The beam path inside the septum magnet is shown in Figure 7.

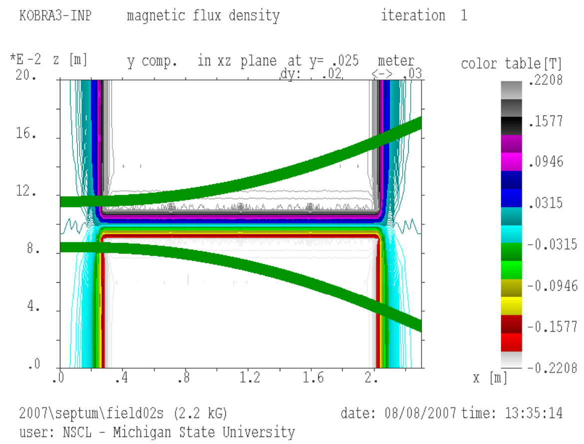


Figure 7: The path of the two separated bunches and the magnetic field distribution in the septum magnet.

The smearing of the beam due to fast amplitude variation of the RF field in the kicker (jitter) will lead to an additional emittance growth. This additional growth, however, is several times smaller than the static growth. The effect of the corresponding RF phase jitter on the final beam emittance for all three phase space projections was found to be negligible in all simulations.

## CONCLUSION

A proposed FRIB beam switchyard using an RF kicker and magnetic septum system to split the beam into two downstream beam lines on a micro-bunch by micro-bunch basis provides high quality beam on targets. It is possible to enhance the efficacy of this system by differentially loading the micro-bunches by employing a system in the Medium Energy Beam Transport system.

A dc septum system consisting of an array of thin wires and two cathodes could be used to split the beam but only for oxygen ions or lighter.

## REFERENCES

[1] D. Gorelov, T. Grimm, W. Hartung, F. Marti, H. Podlech, X. Wu and R.C. York, “Beam Dynamics Studies at NSCL of the RIA Superconducting Driver Linac”, proc. of EPAC 2002, Paris, France, 2002.

[2] M. Doleans, V. Andreev, X. Wu R. C. York, “Beam Distribution System for the MSU-RIA Driver Linac”, proc. of LINAC 2006, Knoxville, TN, USA, 2006.

[3] D.V.Gorelov and P.N.Ostroumov, “Applications of the LANA Code for Design of Ion Linacs”, Proc. of the EPAC’96 Conf., Sitges, Spain, (1996) p.1271.